Received April 2001
Revised 2002
Accepted May 2002

Vortex shedding over a rectangular cylinder with ground effect: flow and heat transfer characteristics

S.Z. Shuja, B.S. Yilbas and M.O. Budair
ME Department, KFUPM, Dhahran, Saudi Arabia

Keywords *Vortex shedding, Heat transfer*

Abstract *The vortex shedding from a rectangular cylinder improves the heat transfer rates. Introducing a ground effect in such a flow system alters the shedding frequency, which in turn enables to vary the cooling rates of the cylinder. In the present study a laminar flow passing over a rectangular cylinder with a ground effect is considered. The flow and energy equations are solved numerically using a control volume approach. Strouhal and Stanton number variations due to gap height are computed and the influence of Strouhal number on Stanton number variation behind the cylinder is examined. The study is extended to include the predictions of entropy generation in the solution domain. It is found that shedding frequency increases as gap height reduces and further reduction in gap height results in diminishing of vortex shedding, in which case confined flow is developed in the gap. Heat transfer rates improve when Strouhal number is maximum. In the case of confined flow situation, heat transfer rates enhance substantially in the region close to the top corner of the cylinder, in which case, non-uniform cooling of the surface is resulted.*

Nomenclature

α_f	= heat diffusivity of fluid, m^2/s	ρ_f	= density of fluid, kg/m^3
B	= height of rectangular cylinder, m	ρ_s	= density of solid, kg/m^3
c_{p_f}	= specific heat for fluid, J/kgK	Re	= Reynolds number
c_{p_s}	= specific heat for solid, J/kgK	S	= Strouhal number
Ec	= Eckert number	S_{int}	= dimensionless time integrated entropy
Fo	= Fourier number	S_{gen}	= dimensionless entropy generation
k_f	= thermal conductivity of fluid, W/mK	S'''_{gen}	= entropy generation rate, W/m^3K
k_s	= thermal conductivity of solid, W/mK	St	= Stanton number
l	= dimensionless gap height	t	= dimensionless time
l^*	= gap height (distance between cylinder and ground), m	t^*	= time, s
n^*	= distance in the direction normal to the wall surface	t_b	= dimensionless time when shedding reaches steady
P	= dimensionless pressure	T	= dimensionless temperature
P^*	= pressure, Pa	T^*	= temperature, K
Pr	= Prandtl number	T_f	= dimensionless fluid temperature
q	= dimensionless heat flux	T_f^*	= fluid temperature, K
q'''	= heat flux, W/m^3		

International Journal of Numerical Methods for Heat & Fluid Flow, Vol. 12 No. 8, 2002, pp. 916-939.

DOI 10.1108/09615530210448705

The authors acknowledge the support of King Fahd University of Petroleum and Minerals, Dhahran, Saudi Arabia, for this work.

T_g = dimensionless ground temperature (wall temperature of ground)
T_g^* = ground temperature (wall temperature of ground), K
T_i^* = inlet temperature, K
T_0^* = initial temperature, K
T_s = dimensionless solid temperature
T_{s*} = solid temperature, K
T_w = wall temperature, K
u = dimensionless axial velocity
u^* = axial velocity, m/s
u_0 = inlet velocity (upstream velocity), m/s
v = dimensionless velocity along y-axis
v^* = velocity along y-axis, m/s
ν_f = viscosity of fluid, m^2/s
x = dimensionless distance along x-axis
x^* = distance along x-axis, m
y = dimensionless distance along y-axis
y^* = distance along y-axis, m

1. Introduction

Vortex shedding is an unsteady flow structure that is generated behind relatively slender, bluff bodies. The heat transfer characteristics of the bluff body highly depends on the flow structure developed around it. The investigation into flow structure and heat transfer characteristics of a bluff body subjected to vortex shedding is fruitful in many engineering applications.

Incompressible flow around bluff body is a phenomenon, which is studied extensively both numerically and experimentally. An optimum suppression of fluid forces by controlling a shear layer separated from a square prism was investigated by Sakamoto *et al.* (1991). The control of the separated shear layer was established by setting up a small circular cylinder on one side of the body. They showed that the fluid forces and the frequency of vortex shedding of the square prism were mainly dependent on the characteristics of a very thin region near the outer boundary of the shear layer. The numerical simulations of vortex shedding past a free-standing square cylinder was carried out by Bosch and Rodi (1998). They showed that the choice of the inflow location and the inflow conditions had a significant influence on the predictions. A numerical study of vortex shedding from a square cylinder with ground effect was investigated by Hwang and Yao (1997). They computed drag and lift coefficients numerically. They demonstrated that the presence of the wall had strong effects on the properties of the vortices as well as lift, drag and Strouhal number. The behavior of the secondary vortex during a vortex-wedge interaction was investigated by Park and Lee (1999). They demonstrated that within the distance of the incident vortex diameter, the maximum strength of the secondary vortex was almost constant, and convection velocities showed linear trends with the vertical distance changed. The influence of no-slip boundary condition on the numerical simulation of two-dimensional incompressible flow past a circular cylinder was investigated by Pinol and Grau (1998). They indicated that an accurate prediction of mean coefficients and their amplitudes required a fine description of the cylinder wall.

When a bluff body is subjected to a vortex shedding, heat transfer characteristics of the body changes considerably. This is because of the improved mass transfer rates from the surface in the region affected by a vortex shedding. Considerable research studies were carried out to explore the heat transfer characteristics of a bluff body subjected to a vortex shedding. Turbulent heat transport in a boundary layer behind a junction of a streamlined cylinder and a wall was investigated by Wroblewski and Eibeck (1992). They showed that peak values of the Stanton number and the eddy diffusivity were observed in the inner-wake region, where the cross-spectra of turbulent heat flux did not exhibit a peak near the shedding frequency, but did show an increase compared to a two-dimensional boundary layer over a much broader frequency range. A laminar mixed convection from a circular cylinder using a body-fitted coordinate system was investigated by Chen *et al.* (1994). They showed that with an increase of Grashof number, the point of separation moved upward and the isothermal pattern changed accordingly. Heat and mass transfer from a circular cylinder exposed to a convective environment with a surface reaction of arbitrary order was studied by Nguyen *et al.* (1996). They indicated that the shedding phenomena caused the temperature along the surface of the cylinder to be elevated, which in turn lead to higher heat transfer rates. The effect of large-scale periodic unsteadiness on the heat transport in the downstream region of a junction boundary layer was investigated by Wroblewski (1996). He indicated that vortex shedding from the obstacle could greatly affect the heat transport downstream of the junction. The heat transfer on the base surface of three dimensional protruding elements was studied by Chyu and Natarajan (1996). They showed that the convective transport was largely dominated by the formation of the upstream vortex system as well as the wake vortices downstream to the element. The heat transfer characteristics of flow past a rectangular protruding body was investigated by Shuja *et al.* (2000). They demonstrated that the relative heat transfer rates improved considerably, whereas relative irreversibility ratio became less for unsteady flow as compared to that obtained from the steady flow. Fluid flow and heat transfer around a cylindrical protuberance mounted on a flat plate boundary layer was studied by Tsutsui *et al.* (2000). They indicated that the results obtained for averaged heat transfer coefficient agreed well with the experimental findings. Steady and unsteady forced convection past an inclined elliptic cylinder was investigated by D'Alessio (1997). He showed that the main role of rotation was to cause fluctuations in the temporal variation of Nusselt number and to distort the thermal tail region emanating from the near tip of the ellipse.

In flow and heat transferring systems, entropy is generated due to fluid friction and heat transfer. The entropy generation in a thermal system provides useful information on the irreversibility associated within the system. Considerable research studies were conducted to determine the irreversibility

associated with a thermal system and minimize the system losses for improved design and operation. A review on entropy generation minimization was presented by Bejan (1996). The review introduced development and adoption of methods in several areas of engineering disciplines. Entropy generation in conjugate heat transfer from a discretely heated plate to an impinging confined jet was studied by Ruocco (1997). He showed that in the thermal system, the integrated entropy generation rate increased with the thermal conductivity ratio whereas the plate length-averaged Nusselt number did not depend on the thermal conductivity ratio. The entropy generation in laminar convection from an isothermal cylinder in cross flow was examined by Abu-Hijleh (1998). He showed that a significant increase in entropy generation occurred due to mixed convection over pure forced convection, especially at small cylinder diameters. An entropy generation for mixed convective flows in a vertical channel with transverse fin array was studied by Cheng *et al.* (1994). They suggested that a relation existed between the geometric configuration of channel and entropy generation. Second law analysis of combined heat and mass transfer in internal and external flows was examined by Carrington and Sun (1992). They argued an existence of a spurious coupling between heat and mass transfer that influenced the entropy production rate.

The vortex shedding was shown to enhance considerably the Stanton number behind the bluff body (Shuja *et al.*, 2000). Moreover, control of vortex shedding is possible by imposing a ground effect on the flow field. In this case, shedding frequency and the amplitude of pressure oscillation vary depending on the location of a ground from the bluff body. Consequently, investigation into the flow and heat transfer characteristics of a bluff body with ground effect is necessary. In the present study, a rectangular two-dimensional cylinder located away from the solid wall (ground) subjected to a laminar flow is considered. The governing equations of flow and energy are solved numerically using a control volume approach. The heat transfer characteristic due to the ground effect are presented in terms of non-dimensional quantities. The study is extended to include entropy analysis due to fluid friction and heat transfer.

2. Mathematical analysis

The flow conditions considered is a two-dimensional incompressible flow around a heat generating rectangular cylinder. The geometric arrangement of flow conditions and the cylinder is shown in Figure 1(a). A uniform flow passing over a flat plate is assumed at inlet to the control volume. The two-dimensional Navier-Stokes and continuity equations for unsteady incompressible viscous flow are employed to simulate the flow conditions, while the two-dimensional transient energy and conduction equations are used to obtain the temperature field in the control volume.

The continuity equation in dimensionless form is:

$$\frac{\partial u}{\partial x}+\frac{\partial v}{\partial y}=0$$

The x-momentum equation in dimensionless form is:

$$\frac{\partial u}{\partial t}+u\frac{\partial u}{\partial x}+v\frac{\partial u}{\partial y}=-\frac{\partial P}{\partial x}+\frac{1}{\mathrm{Re}}\left(\frac{\partial^2 u}{\partial x^2}+\frac{\partial^2 u}{\partial y^2}\right)$$

The y-momentum equation in dimensionless form is:

$$\frac{\partial v}{\partial t}+u\frac{\partial v}{\partial x}+v\frac{\partial v}{\partial y}=-\frac{\partial P}{\partial y}+\frac{1}{\mathrm{Re}}\left(\frac{\partial^2 v}{\partial x^2}+\frac{\partial^2 v}{\partial y^2}\right)$$

The energy equation in dimensionless form is:

$$\frac{\partial T}{\partial t}+u\frac{\partial T}{\partial x}+v\frac{\partial T}{\partial y}=\frac{1}{\mathrm{Pr}\,\mathrm{Re}}\left(\frac{\partial^2 T}{\partial x^2}+\frac{\partial^2 T}{\partial y^2}\right)+2\frac{\mathrm{Ec}}{\mathrm{Re}}\left\{2\left[\left(\frac{\partial u}{\partial x}\right)^2+\left(\frac{\partial v}{\partial y}\right)^2\right]+\left(\frac{\partial u}{\partial y}+\frac{\partial v}{\partial x}\right)^2\right\}$$

with the following dimensionless variables:

$$x=\frac{x^*}{B};\ y=\frac{y^*}{B};\ l=\frac{l^*}{B};\ t=\frac{t^* u_0}{B};\ P=\frac{P^*}{\rho_{\mathrm{f}} u_0^2};\ T=\frac{T^*-T_{\mathrm{i}}^*}{T_{\mathrm{w}}^*-T_{\mathrm{i}}^*};\ u=\frac{u^*}{u_0}$$

$$v=\frac{v^*}{u_0};\ \mathrm{Re}=\frac{u_0 B}{\nu_{\mathrm{f}}};\ \mathrm{Pr}=\frac{\nu}{\alpha_{\mathrm{f}}};\ \mathrm{Ec}=\frac{1}{2}\frac{u_0^2}{C\mathrm{p}_{\mathrm{f}}(T_{\mathrm{w}}^*-T_{\mathrm{i}}^*)};\ \mathrm{Fo}=\frac{\alpha_{\mathrm{s}} t^*}{B^2}$$

$$S=\frac{nB}{u_0};\ \mathrm{St}=\frac{q_{\mathrm{w}}}{\rho c_{\mathrm{p_f}} u_0\left(T_{\mathrm{w}}^*-T_{\mathrm{i}}^*\right)};\ S_{\mathrm{gen}}=\dot{S}_{\mathrm{gen}}'''\frac{B^2}{k_{\mathrm{f}}};\ q=\frac{q''' t^*}{\rho_{\mathrm{s}} c_{\mathrm{p_s}}(T_{\mathrm{w}}^*-T_{\mathrm{i}}^*)}$$

In the solid:

$$\frac{\partial T}{\partial t}=\mathrm{Fo}\left(\frac{\partial^2 T}{\partial x^2}+\frac{\partial^2 T}{\partial y^2}\right)+q$$

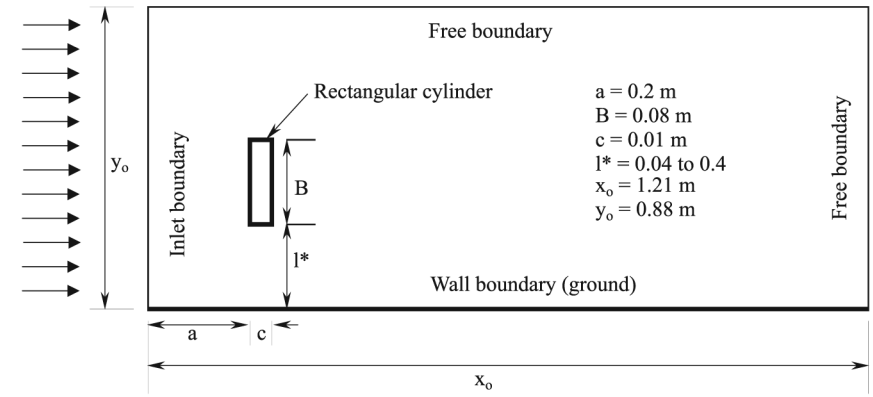

(a)

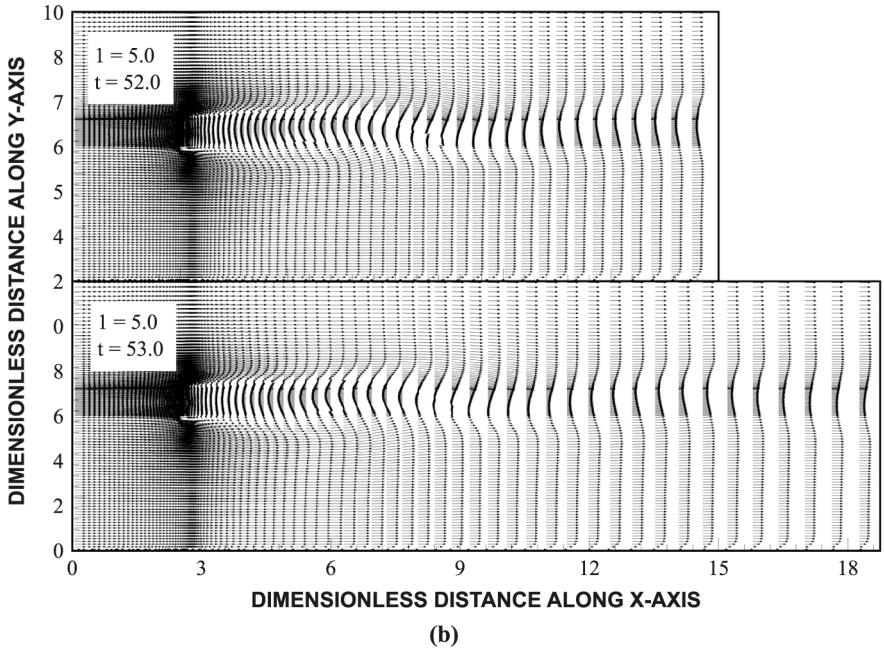

(b)

(*Continued*)

Figure 1.
(a) Schematic view of rectangular cylinder and ground in the solution domain with boundary conditions indicated. (b) Velocity vectors for two downstream lengths from the cylinder and for period at which the pressure is maximum. (c) Variation of maximum Stanton number along the cylinder height for the cases corresponding to two downstream conditions

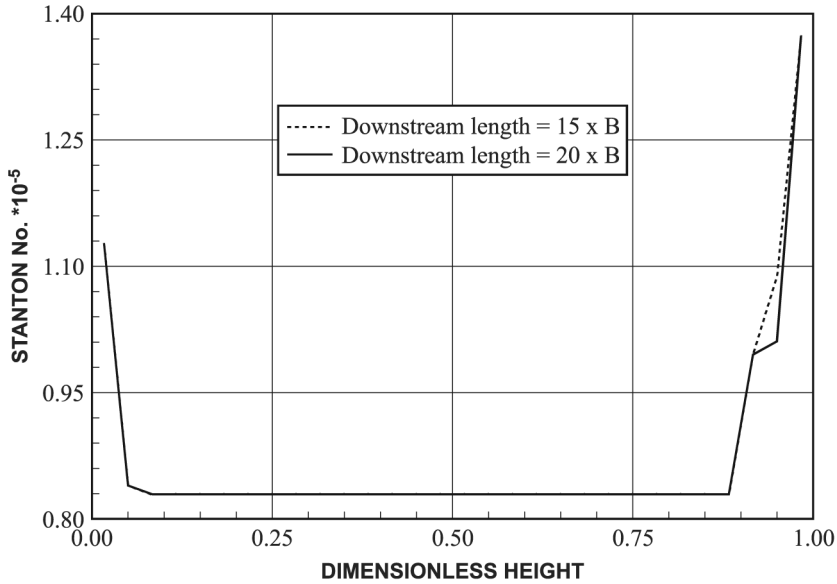

Figure 1.

2.1 Initial and boundary conditions for the flow equations
2..1.1 Initial condition. At $t = 0$

$$u = 1;\ \ v = 0;\ \ T = T_{\mathrm{o}}$$

where

$$T_0 = \frac{T_0^* - T_{\mathrm{w}}^*}{T_{\mathrm{w}}^* - T_{\mathrm{i}}^*}$$

2.1.2 Boundary conditions. At inlet to control volume:

$$u = 1;\ \ v = 0;\ \ T = 0;\ \ P = (\text{specified})$$

At ground (solid wall): (no slip conditions)

$$u = 0;\ \ v = 0$$

At exit to control volume:

$$\text{At } y = \infty;\ \ \frac{\partial \psi}{\partial y} = 0 \text{ and at } x = \infty;\ \ \frac{\partial \psi}{\partial x} = 0$$

where ψ is any of the fluid properties.

2.2 Initial and boundary conditions for the rectangular cylinder and ground
2.2.1 Initial and heating conditions. At $t=0$:

$$T_s = T_0$$

At $t > 0$

$$q = \frac{q''' t^*}{\rho c_{p_s}(T_w^* - T_i^*)}$$

where q''' is the heat input and being specified.

2.2.2 Boundary conditions. When the cylinder is immersed in the boundary layer, the velocity field induced by the vortices is distorted both by the velocity gradient and by the presence of wall. It results in inhibiting the flow development of the wake and modifying the shedding frequency as indicated in the previous studies (Hwang and Yao, 1997; Davis *et al.*, 1984). In order to minimize the effect of velocity gradient due to boundary layer flow, the cylinder is located close to inlet where boundary layer thickness is considerably small. At the solid-fluid interface, continuity of heat flux and temperature is considered:

$$\frac{\partial T}{\partial n^*_s} = \frac{\partial T}{\partial n^*_f}$$

and

$$T_s = T_f$$

where

$$T_s = \frac{T_s^* - T_w^*}{Tw^* - T_i^*}$$

At the ground-fluid interface, continuity of heat flux and temperature is considered:

$$\left|\frac{\partial T}{\partial n^*}\right|_g = \left|\frac{\partial T}{\partial n^*}\right|_f$$

and

$$T_g = T_f$$

where

$$T_g = \frac{T_g^* - T_w^*}{T_w^* - T_i^*}$$

2.3 Entropy analysis

The dimensionless volumetric rate of entropy generation is (Bejan, 1982):

$$S_{gen} = \frac{1}{T^2}\left[\left(\frac{\partial T}{\partial x}\right)^2 + \left(\frac{\partial T}{\partial y}\right)^2\right] + 2\mathrm{Pr}\,\mathrm{Ec}\left\{2\left[\left(\frac{\partial u}{\partial x}\right)^2 + \left(\frac{\partial v}{\partial y}\right)^2\right] + \left(\frac{\partial u}{\partial y} + \frac{\partial v}{\partial x}\right)^2\right\}$$

where S_{gen} is dimensionless entropy generation rate ($S_{gen} = \bar{S}'''_{gen}\frac{B^2}{k_f}$).

The total entropy generation can be obtained through integration of S_{gen} with time, i.e.:

$$S_{tot} = \int_0^{t_b} S_{gen}\mathrm{d}t$$

where t_b is the dimensionless time when the pressure oscillation becomes steady.

The fluid and solid cylinder properties employed in the simulations are given in Table I.

3. Numerical solution

The schematic view of the solution domain is shown in Figure 1(a). For the purpose of solution the flow domain is overlaid with a rectangular grid whose intersection points (nodes) denote the location at which all variables, with the exception of the velocities, are calculated. The latter are computed at locations midway between the pressure which drive them.

Table I. Thermal properties fluid and solid used in the simulation

Re	Pr	Ec	ρ_f kg/m^3	ρ_s kg/m^3	ν m^2/s	k_f W/mK	k_s W/mK	Cp_f J/kgK	Cp_s J/kgK
460	1.14	2×10^{-5}	1.89	7836	1.544×10^{-5}	0.02565	28.2	1005	969

The control volume approach is used in the numerical scheme. A staggered grid arrangement provides handling the pressure linkages through the continuity equation and is known as the SIMPLE algorithm (Patankar, 1980). This method is an iterative process to steady-state convergence. The pressure link between continuity and momentum is accomplished by transforming the continuity equation into a Poisson equation for pressure. The Poisson equation implements a pressure correction for a divergent velocity field. The steady-state convergence is achieved by successively predicting and correcting the velocity components and the pressure. An initial guess for the pressure variable at each grid point is introduced.

The grid independent tests are carried out to ensure the grid independent results; consequently, the grid size and the grid orientation giving the grid independent results are selected, i.e. the mesh used in the present study have 11,700 (90×130) node points.

In order to examine the effect of downstream length from the solid object on the simulation results, downstream length is increased to 20 times of the solid object height ($20 \times B$). The resulting velocity vectors corresponding to downstream lengths of $15 \times B$ and $20 \times B$ are shown in Figure 1(b). It can be seen that the velocity vectors are almost identical, especially in the region of the solid object. Moreover, to investigate the influence of downstream length on Stanton number along the solid object height, Figure 1(c) is plotted. The Stanton numbers corresponding to downstream lengths of $15 \times B$ and $20 \times B$ are almost identical. Consequently, the outlet boundary condition $\partial\phi/\partial x = 0$ is considered at $15 \times B$. To validate the present predictions, the range of Strouhal numbers resulted from the present and previous studies (Hwang and Yao, 1997) for various ground height ratios ($1.3 \leq l \leq 5.0$) is given in Table II. It can be seen that both results are in good agreement.

4. Results and discussions

A numerical simulation of flow past a heat generating rectangular cylinder with ground effect is carried out. The velocity and temperature fields in the solution domain are computed. The influence of ground wall on the Stanton number variation along the height behind the cylinder is examined. The entropy

Table II. Comparison of range of Strouhal numbers corresponding to present and previous studies (Hwang and Yao, 1997)

	Range of ground height ratio	Range of Strouhal number
Previous study	$1.0 \leq l \leq 8.0$	$0.084 \leq S \leq 0.140$
Present study	$1.3 \leq l \leq 5.0$	$0.108 \leq S \leq 0.139$

generation due to fluid friction and heat transfer is computed. The fluid and solid properties employed in the simulations are given in Table I. The velocity vectors, axial velocity component, temperature and entropy contours are plotted when the pressure in the region close to the top corner behind the cylinder is maximum and minimum. This is because of the high magnitude of pressure oscillation due to vortex shedding in this region. The time periods corresponding to maximum and minimum amplitudes of pressure oscillation are considered to represent comprehensively the change in flow and heat transfer characteristics in the solution domain; therefore, these time periods are selected to present the predictions. It should be noted that the rectangular cylinder is placed closed to the inlet of the control volume. This arrangement avoids the influence of the upstream boundary layer flow on the flow and heat transfer characteristics around the cylinder.

Figure 2 shows the velocity vectors for different gap heights (spacing between the cylinder and ground). The velocity vectors are plotted for the situations when the pressure in the region next to the top corner behind the cylinder is maximum and minimum. The stagnation region is developed in the frontal surface of the cylinder and due to velocity gradient, flow expansion from top and bottom corners of frontal surface is evident. In the case of free stream flow ($l = 5$, almost no ground effect), the vortex shedding corresponding to maximum and minimum pressures have same frequency and amplitude provided that they are out of phase. As the gap height (distance between the cylinder and ground) reduces (body becomes close to the ground), the velocity field induced by the vortices is distorted by the presence of ground, i.e. it results in inhibiting the flow development of wake and influencing the shedding frequency. The presence of ground results in the formation of circulation cell behind the body in the region close to the ground. In this case, the reattachment effects the wake flow.

Figure 3 shows the axial velocity contours for different gap height and when pressure in the region close to the top corner behind the cylinder is maximum and minimum. In the case of large gap height ($l = 5$), a large circulation cell behind the cylinder is formed, since the shedding occurs out of phase and the shear flow generates a large circulation cell. The structure of the circulation cell changes with the orientation of the vortices. As the gap height reduces, the shedding frequency increases. The decrease in the gap height results in a situation that occurs in confined flow with blockage effect, in which case, the flow between the cylinder and the ground is accelerated. As the gap height decreases further the shedding diminishes due to the presence of secondary stationary cell behind the cylinder, i.e. two circulation cells with opposite rotations are generated behind the body. The generation of the second cell is because of the shear effect of the accelerated flow in the gap between the cylinder and the ground. Moreover, the confined flow results in initiation of reverse flow above the ground in the downstream. This suppresses

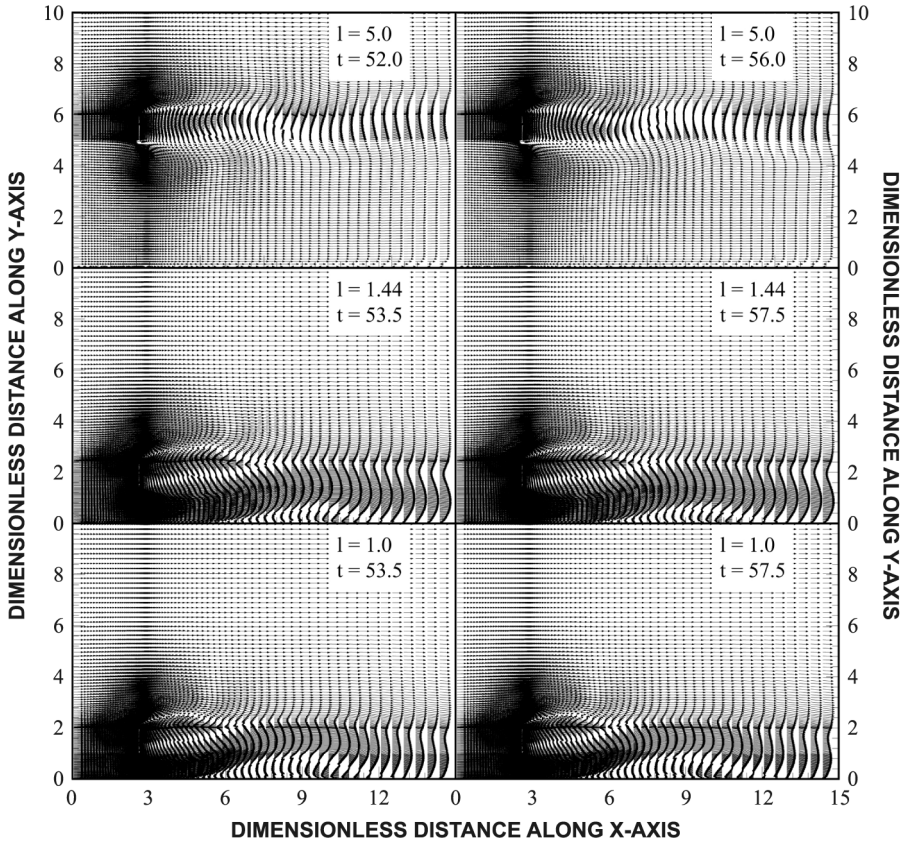

Figure 2.
Velocity vectors at different gap height ratios and for periods at which pressures are maximum and minimum

the detachment of the cells behind the cylinder. Consequently, the shedding replaces flow expansion from the top corner and accelerated confined flow from the bottom corner behind the cylinder. This occurs at gap height $l = 1.375$ in the present simulation conditions. This situation is also reported for the case of thin boundary layer in the previous study (Hwang and Yao, 1997). Moreover, the critical gap, where vortex shedding ceases, increases to about 2.5 times of the present case for the circular cylinders (Zdravkovich, 1981; Okajima, 1979).

Figure 4 shows the temperature contours for different gap height and when the pressure close to the top corner behind the cylinder is maximum and minimum. Temperature contours follow almost the velocity contours including the circulation cells. Temperature contours are denser near the top and bottom corners behind the cylinder. This indicates that convective cooling of the cylinder surface is considerably high in these regions. Moreover, convective cooling in the mid region of the surface is low. This is because of the circulation cell generated behind the cylinder, i.e. counter-rotating cells sweep the heated

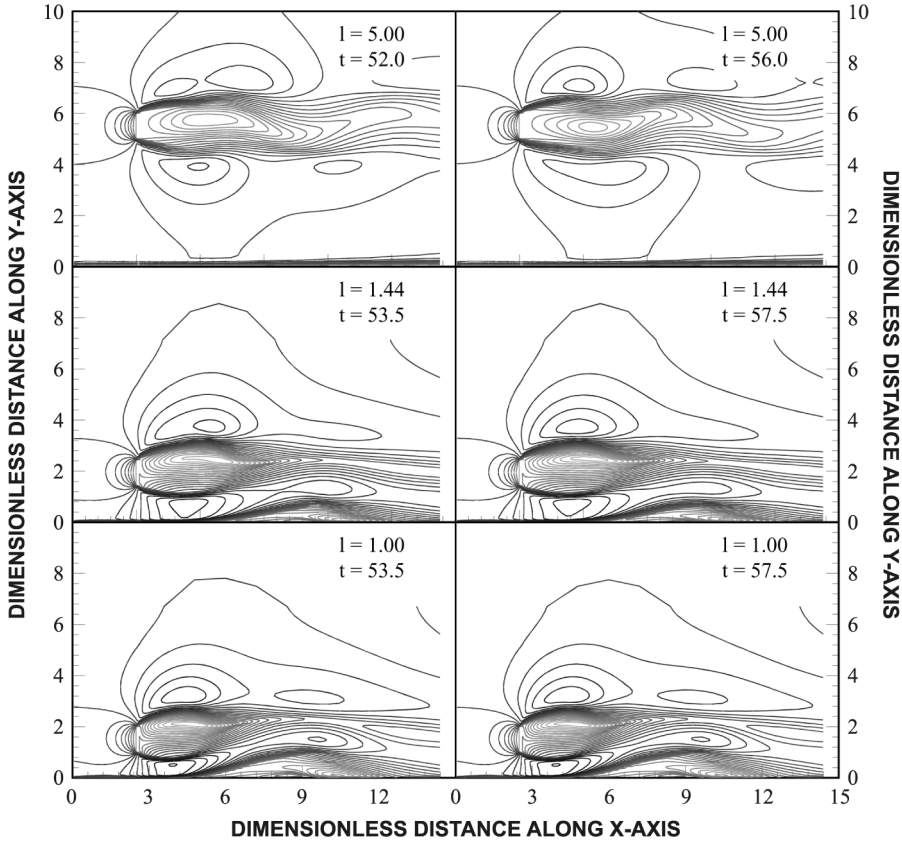

Figure 3.
Axial velocity contours at different gap height ratios and for periods at which pressures are maximum and minimum

fluid away from the wall at a slow rate. This, in turn, results in a high temperature attainment in the central region of the surface. As the gap height reduces, the influence of blockage effect on temperature distribution due to confined flow situation becomes significant. In this case, temperature contours extend further into the downstream of the flow. Since, the second circulation behind the cylinder is stationary, a high temperature region is developed in this region. Further away from the cylinder, the fluid temperature reduces because of the mixing of the flow in the downstream.

Figure 5 shows three-dimensional plot of Stanton number variation along the height behind the cylinder with time for different gap height. Stanton number represents mainly the heat transfer rates, therefore, high Stanton number represents the high convective heat transfer rates. Stanton number oscillates at a constant frequency and amplitude at top and bottom corners of the cylinder, provided that oscillation is out of phase at top and bottom corners.

This is because of the shedding from these corners. As the gap height reduces, the frequency and amplitude of Stanton number oscillation reduces due to the blockage effect of the confined flow as consistent with the previous study for thin boundary layer case. Moreover, Stanton number corresponding to bottom corner attains lower values as compared to its counterpart corresponding to top corner. The blockage effect enhances the shedding frequency and results in flow expansion from the top corner of the cylinder as reported by Davis *et al.* (1984) and Mukhopadhyay *et al.* (1992). This, in turn, enhances the convective heat transfer from the top corner of the cylinder. As the gap height reduces further, Stanton number in the top and bottom corners increases, provided that increase in Stanton number is more pronounced in the top corner. Although shedding diminishes at the gap height considered, the expansion of fluid from the top corner and the flow accelerates in gap between the cylinder and ground due to the confined flow situation improve the convective heat transfer in this region.

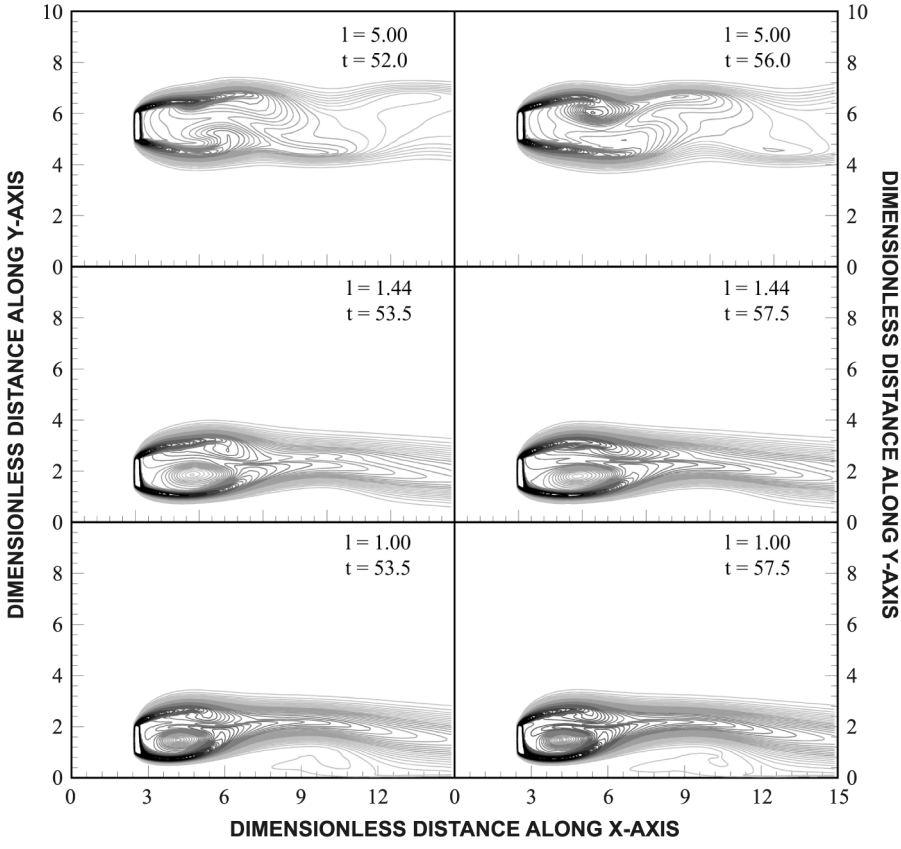

Figure 4.
Temperature contours at different gap height ratios and for periods at which pressures are maximum and minimum

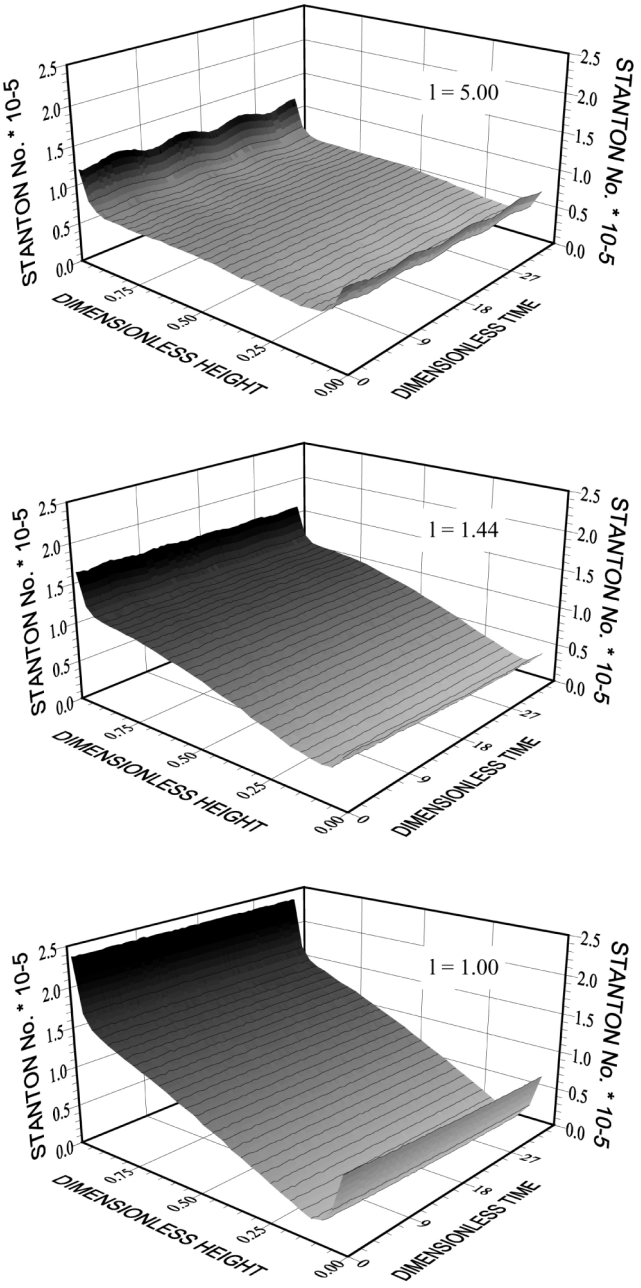

Figure 5.
Stanton number variation along the cylinder height with time for three gap height ratios

Figure 6 shows the time averaged Stanton number variation behind the cylinder. Stanton number improves as gap height reduces while the distance along the surface behind the cylinder approaches to top corner. Moreover, the enhancement becomes considerable as the gap height reduces to $l = 1.375$, in which case shedding diminishes. The non-uniform distribution of Stanton number along the cylinder height is because of the circulation cells developed behind the cylinder, i.e. the strength and the size of circulation cells effect the Stanton number distribution. This is more pronounced as the gap height becomes small. In this case, non-uniform convective cooling of the back surface of the cylinder is resulted.

Figure 7 shows the Stanton number variation behind the cylinder when Strouhal number (S) is maximum and minimum. This provides information on the effect of S on the heat transfer rates, i.e. depending on the gap height, S attains maximum and minimum and Stanton number distribution along the cylinder height varies with respect to S. It should be noted that the maximum Stanton number in whole time domain is plotted in Figure 7. The influence of S on Stanton number is less significant in the region close to the bottom corner of the cylinder. Stanton number increases sharply as the distance from mid height increases towards the top corner of the cylinder, which is true for large S. However, the influence of Stanton number does not vary considerably along the body height for small S, except the corners. Increasing S, therefore, influences considerably the Stanton number distribution along the cylinder height. This indicates that increasing mass removal rate close to the top corner through high frequency shedding enhances the heat transfer rates from this region.

Figure 8 shows Strouhal number and the normalized pressure behind the body with gap height. The pressure is normalized with the maximum pressure behind the cylinder. S increases with decreasing gap height. In this case, the velocity in the gap between the cylinder and the ground increases similar to that occurs in the confined flow due to blockage effect. Moreover, with decreasing gap height, blockage ratio increases, which in turn results in increasing S as noted by Davis *et al.* (1984) and Mukhopadhyay *et al.* (1992). As the gap height decreases further, the wake behind the cylinder becomes stationary and shedding diminishes. The pressure behind the cylinder reaches its minimum when vortex shedding diminishes. Increasing gap height results in increasing pressure amplitude reaching its maximum. This is due to the orientation of vortices behind the cylinder; in which case, the orientation of vortices is modified with the presence of the ground. Moreover, pressure oscillation behind the cylinder settles as the gap height increases further. In this case the blockage effect becomes insignificant.

Figure 9 shows the Stanton number variation with gap height at top and bottom corners and mid height behind the cylinder. Stanton number is affected by the gap height. This is more pronounced for small gap heights. Moreover, influence of vortex shedding from the bottom corner of the cylinder is

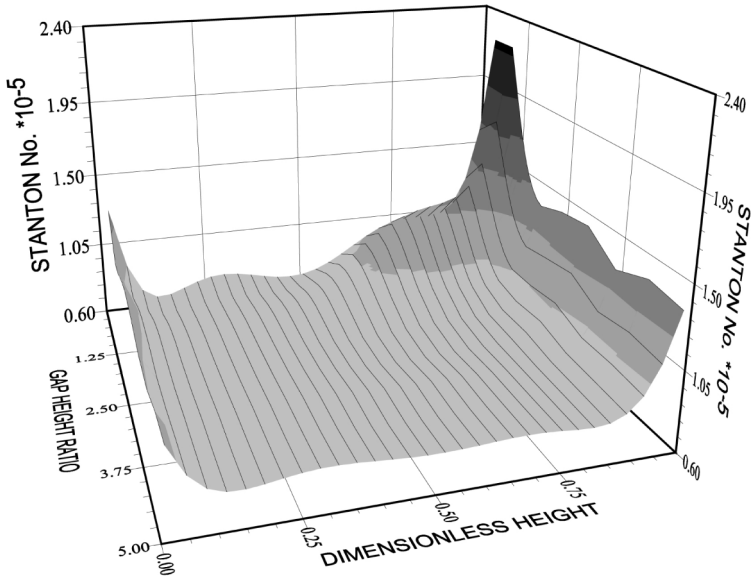

Figure 6.
Variation of maximum Stanton number along the cylinder height and gap height ratio

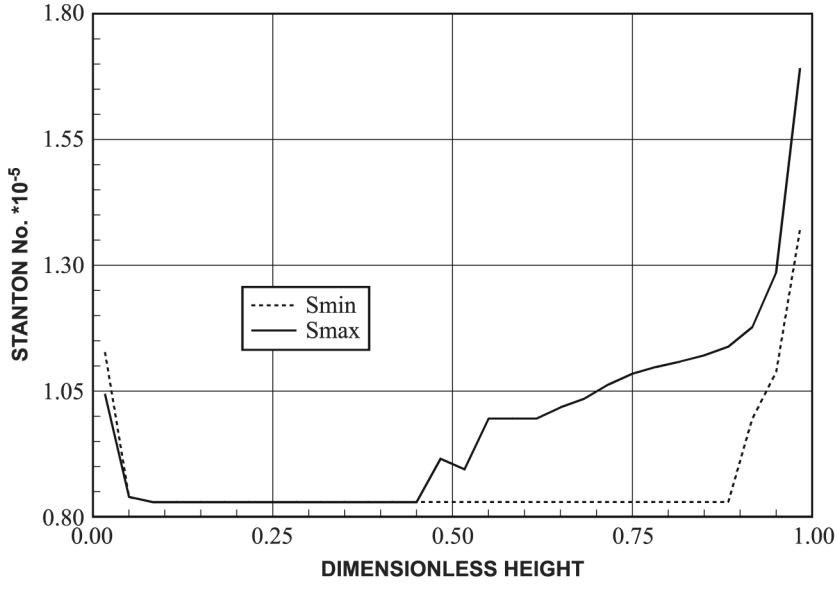

Figure 7.
Variation of maximum Stanton number along the cylinder height for the cases corresponding to maximum and minimum Strouhal numbers

considerable. In this case, Stanton number improves considerably, at top corner of the cylinder, for gap heights of 1.38-2.

Figure 10(a) and (b) shows the three-dimensional plots of entropy generation due to fluid friction and heat transfer with gap height and time. Entropy surface due to heat transfer increases with time while its variation with gap height is almost uniform, except for small gap heights, in which case it increases slightly. The increase in entropy generation rate is due to improved heat transfer rates at small gap heights. In the case of Figure 10(b), entropy generation due to fluid friction remains almost uniform with time except at long heating periods, in which case entropy production reduces slightly for small gap heights. Entropy production, however, increases sharply with gap height for all heating durations. The sharp increase of entropy with reducing gap height is because of the frictional losses generated due to blockage effect in the confined flow situation. The behavior of frictional entropy generation is different than its counterpart corresponding to heat transfer. This suggests that (1) the frictional loss is more pronounced as gap height reduces, and (2) temperature gradient in the flow field increases as the heating period progresses.

Figures 11 and 12 show the variation of time integrated entropy generation due to heat transfer and fluid friction with gap height. The entropy generation due to heat transfer and fluid friction is higher for small gap heights. In this case, frictional losses and temperature gradient in the flow field becomes high. The secondary peak in entropy generation due to heat transfer is observed in

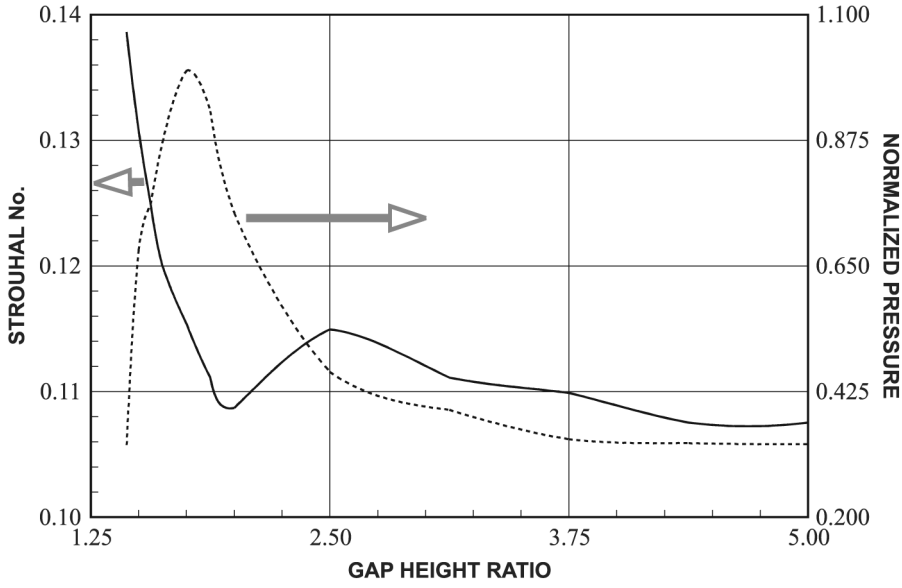

Figure 8.
Strouhal number and normalized pressure (P/P_{max}) variations with gap height ratio

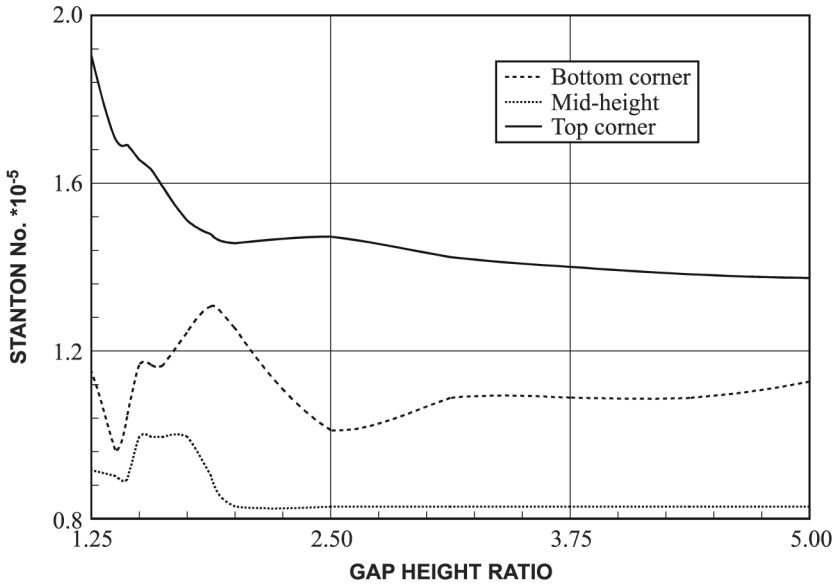

Figure 9.
Variation of maximum Stanton number with gap height ratio for three locations along the cylinder height

the region where the shedding is diminished. This, however, results in almost uniform entropy generation due to fluid friction in this region. This occurs because of the complex flow structure generated in the region where the vortex shedding diminishes. In this case, heat transfer improves locally while fluid friction does not alter considerably.

5. Conclusions

Vortex shedding with a ground effect due to rectangular cylinder is studied for various gap heights. The flow and heat transfer characteristics are computed numerically and the cylinder geometric parameters are kept constant during the simulations. Entropy generation due to heat transfer and fluid friction is computed to account for the entropic losses in the flow system. It is found that the shedding frequency increases as the gap height reduces, which is due to the blockage effect and generation of confined flow situation between the cylinder and the ground. Heat transfer characteristics along the height behind the cylinder improve considerably as shedding frequency increases. Moreover, heat transfer rates enhances further as shedding diminishes, in which case non-uniform cooling of the surface behind the cylinder is resulted. The specific conclusions derived from the present work are listed as follows.

(1) A large circulation cell is developed behind the cylinder during the vortex shedding due to the shear layer interactions in this region. The orientation

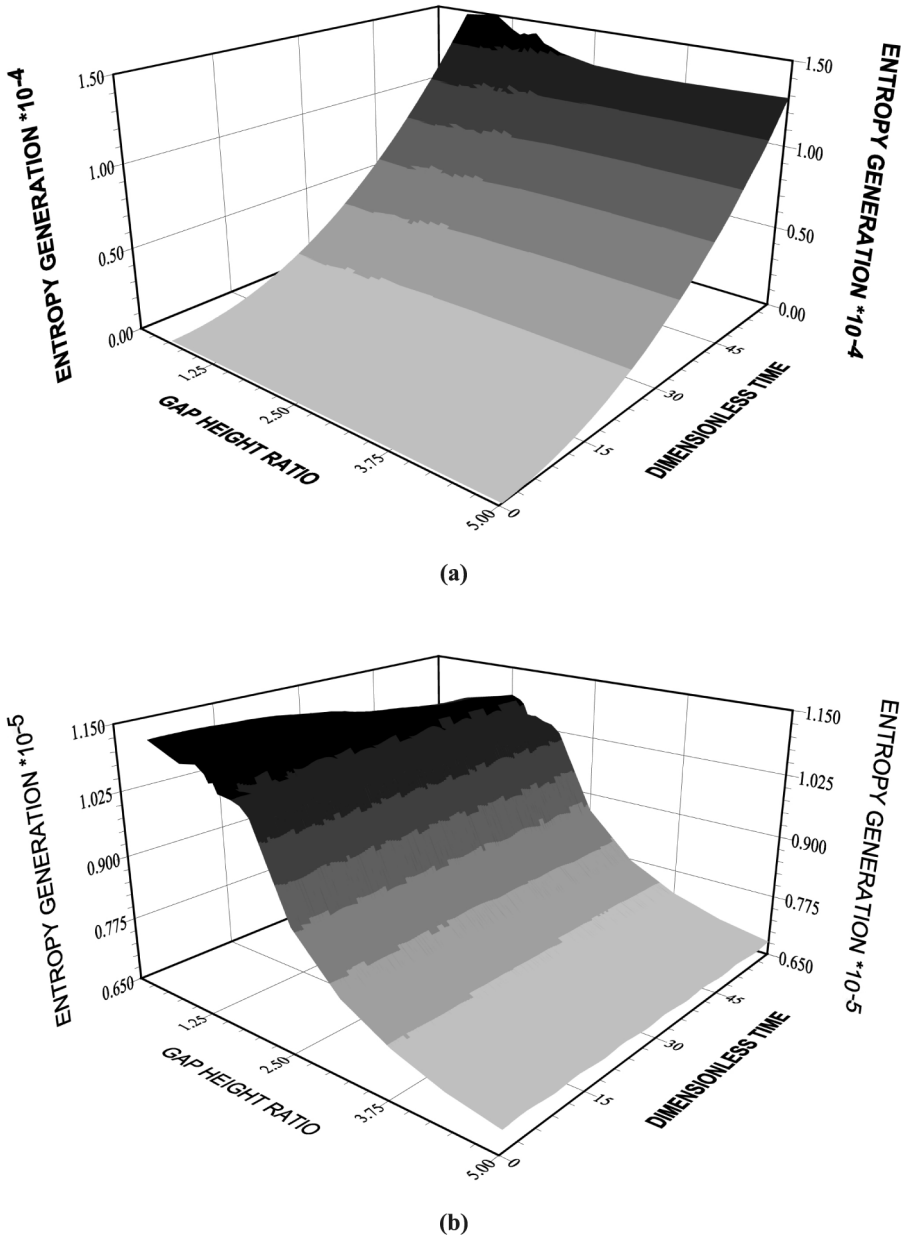

Figure 10.
(a) Dimensionless entropy generation due to heat transfer. (b) Dimensionless entropy generation due to fluid friction

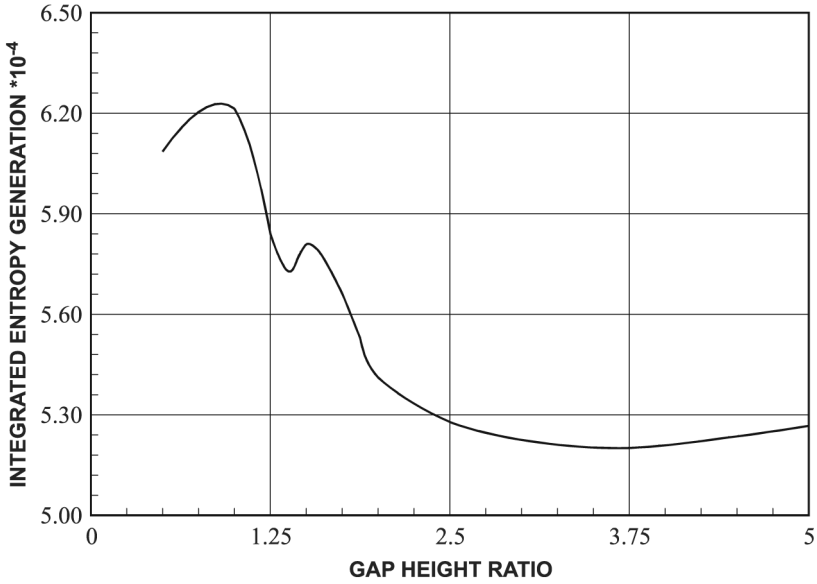

Figure 11.
Variation of time integrated entropy generation due to heat transfer with gap height ratio

and size of the circulation cell change with time depending on the orientation of vortices. As the gap height reduces, the shedding frequency increases because of the blockage effect and confined flow development in the gap between the cylinder and the ground. When the gap height

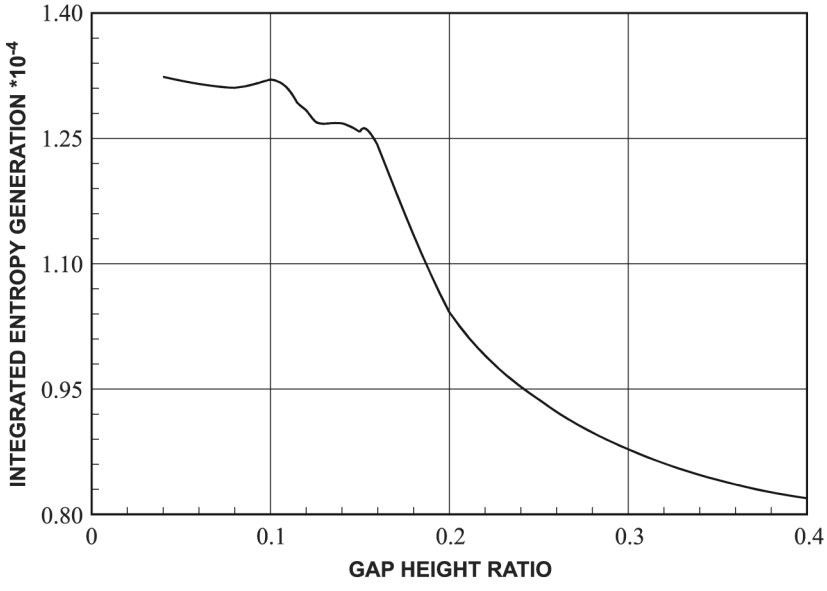

Figure 12.
Variation of time integrated entropy generation due to fluid friction with gap height ratio

reduces further shedding diminishes and standing circulation cells are resulted due to the reverse flow in the downstream.

(2) Temperature contours follow almost velocity contours behind the cylinder. Temperature contours extend coherently from the top and bottom corners of the cylinder towards the downstream. In this case, temperature attains high values in these regions. Due to the circulation cells behind the body, temperature contours follow the flow field and does not extend coherently towards the downstream. Further away from the cylinder surface, fluid temperature reduces because of the mixing of the flow in the downstream.

(3) Stanton number oscillates, with constant frequency and amplitude, in the region close to the top and bottom corners behind the cylinder. As the gap height reduces, the oscillation frequency increases while amplitude of oscillation reduces. Moreover, Stanton number attains higher values in the region close to the top corner as compared to its counterpart corresponding to the bottom corner. As the gap height increases further, shedding diminishes and Stanton number becomes steady and it increases substantially towards the top corner.

(4) Stanton number increases sharply from the mid-height towards the top corner when Strouhal number is maximum. Moreover, Stanton number distribution along the height behind the cylinder does not change, except in the top and bottom corner vicinities, when Strouhal number is minimum. This suggests that at high shedding frequency, mass removal rate along the surface behind the cylinder improves considerably, which in turn enhances the heat transfer rates in this region.

(5) Entropy generation due to heat transfer increases with advancing heating period while entropy generation due to fluid friction increases as gap height reduces. This indicates that frictional loss enhances as the gap height reduces and temperature gradient increases as heating period progresses. Moreover, the total entropy generation due to fluid friction and heat transfer enhances considerably for small gap heights, i.e. the temperature gradient in the flow field and frictional loss amplify as gap height reduces.

References

Abu-Hijleh, B.A.K. (1998), "Entropy generation in laminar convection from an isothermal cylinder in cross flow", *Energy*, Vol. 23 No. 10, pp. 851-7.

Bejan, A. (1982), *Entropy generation through heat and fluid flow*, John Wiley and Sons, New York.

Bejan, A. (1996), "Entropy generation minimization: the new thermodynamics of finite-size devices and finite-time processes", *Journal of Applied Physics*, Vol. 79 No. 3, pp. 1191-218.

Bosch, G. and Rodi, W. (1998), "Simulation of vortex shedding past a square cylinder with different turbulence models", *International Journal for Numerical Methods in Fluids*, Vol. 28, pp. 601-16.

Carrington, C.G. and Sun, Z.F. (1992), "Second law analysis of combined heat and mass transfer in internal and external flows", *International Journal of Heat and Fluid Flow*, Vol. 13 No. 1, pp. 65-70.

Chen, C., Yang, Y. and Wu, S. (1994), "Laminar mixed convection from a circular cylinder using a body-fitted coordinate system", *Journal of Thermophysics and Heat Transfer*, Vol. 8 No. 4, pp. 695-701.

Cheng, C., Ma, W. and Huang, W. (1994), "Numerical predictions of entropy generation for mixed convective flows in a vertical channel with transverse fin array", *International Communications in Heat and Mass Transfer*, Vol. 21 No. 4, pp. 519-30.

Chyu, M.K. and Natarajan, V. (1996), "Heat transfer on the base surface of three-dimensional protruding elements", *International Journal of Heat and Mass Transfer*, Vol. 39 No. 14, pp. 2925-35.

D'Alessio, S.J.D. (1997), "Steady and unsteady forced convection past an inclined elliptic cylinder", *Acta Mechanica*, Vol. 123 No. 1-4, pp. 99-115.

Davis, R.W., Moore, E.F. and Purtell, L.P. (1984), "A numerical-experimental study of confined flow around rectangular cylinders", *Physics of Fluids*, Vol. 27 No. 1, pp. 46-58.

Hwang, R.R. and Yao, C. (1997), "A numerical study of vortex shedding from a square cylinder with ground effect", *ASME Journal of Fluids Engineering*, Vol. 119, pp. 512-8.

Mukhopadhyay, A., Biswas, G. and Sundararajan, T. (1992), "Numerical investigation of confined wakes behind a square cylinder in a channel", *International Journal for Numerical methods in Fluids*, Vol. 14, pp. 1473-84.

Nguyen, H.D., Paik, S. and Douglass, R.W. (1996), "Convective transport about cylinder with surface reaction of arbitrary order", *AICHE Journal*, Vol. 42 No. 6, pp. 1514-24.

Okajima, A. (1979), "Flows around two tandem circular cylinders in very high reynolds numbers", *Bulletin of the JSME*, Vol. 22 No. 166, pp. 504-11.

Park, J.H. and Lee, D.J. (1999), "Behavior of the secondary vortex during a vortex-wedge interaction", *AIAA Journal*, Vol. 37 No. 9, pp. 1131-3.

Patankar, S.V. (1980), *Numerical Heat Transfer*, McGraw-Hill, New York.

Pinol, S. and Grau, F.X. (1998), "Influence of the no-slip boundary condition on the prediction of drag, lift and heat transfer coefficients in the flow past a 2-d cylinder", *Numerical Heat Transfer, Part A*, Vol. 34, pp. 313-30.

Ruocco, G. (1997), "Entropy generation in conjugate heat transfer from a discretely heated plate to an impinging confined jet", *International Communications in Heat and Mass Transfer*, Vol. 24 No. 2, pp. 201-10.

Sakamoto, H., Tan, K. and Haniu, H. (1991), "An optimum suppression of fluid forces by controlling a shear layer separated from a square prism", *ASME Journal of Fluids Engineering*, Vol. 113, pp. 183-9.

Shuja, S.Z., Yilbas, B.S. and Iqbal, M.O. (2000), "Heat transfer characteristics of flow past a rectangular protruding body", *Numerical Heat Transfer, Part A*, Vol. 37, pp. 307-21.

Tsutsui, T., Igarashi, T. and Nakamura, H. (2000), "Fluid flow and heat transfer around a cylindrical protuberance mounted on a flat plate boundary layer", *JSME International Journal, Series B*, Vol. 43 No. 2, pp. 279-87.

Wroblewski, D. (1996), "Effect of large-scale periodic unsteadiness on the heat transport in the downstream region of a junction boundary layer", *International Journal of Heat and Fluid Flow*, Vol. 17, pp. 3-11.

Wroblewski, D.E. and Eibeck, P.A. (1992), "Turbulent heat transport in a boundary layer behind a junction of a streamlined cylinder and a wall", *ASME Journal of Heat Transfer*, Vol. 114, pp. 840-9.

Zdravkovich, M.M. (1981), "Review and classification of various aerodynamic and hydrodynamic means for suppressing vortex shedding", *Journal of Wind Engineering and Industrial Aerodynamics*, Vol. 7 No. 2, pp. 145-89.